and carboxyl terminal regions (17, 22, 29). To generate a complementary peptide to the carboxyl terminal of C5a, we employed the software program COMPEP to target the last 10 amino acids at the carboxyl terminal of C5a (ISHKDMQLGR), which we call C5a-decapeptide.

MATERIALS AND METHODS

Design of C-peptides.

The computer program, COMPEP, which employs a genetic algorithm, was used to generate recognition peptides to a peptide target. Each iteration and score was assigned according to different physicochemical parameters including hydropathy (Kyte-Doolittle) (19), bulkiness, and charge.

Several sets of values for bulkiness are available to be chosen in COMPEP. In this experiment we have used the volume of amino acid (28) for calculation. Charge of amino acid is considered by the side-chain acidity. (Table 2)

Description of Genetic Algorithm

The genetic algorithm is an extraordinary computational tool for optimization used in several fields of science and engineering, its main characteristics stemming from natural selection. The three fundamental operations of selection, crossover and mutation which a GA is endowed with operate on sets (population) of solutions (chromosomes) encoded as strings of bits. As for DNA, the four nucleotides are represented as G, C, U, and A; in GA, the bits are represented by 0, 1, 2 and 3 representatively. In this way, as how an amino acid can be coded by the codon table, it can also be coded by strings of bits in the GA.

To initiate the first iteration, a population of 500 individuals was generated randomly. After calculating the scores of the individuals according to the parameters (hydropathy, charge and bulkiness). Individuals were selected for reproduction using roulette wheel selection (21). From these selected individuals (parents), mutation and crossover would also be performed to generate new individuals for the next iteration. After 10000 iterations, individuals with scores larger than 95% of the maximum score would be recorded in the resulting file.

In this study, altogether 25 combinations of parameter scoring were utilized. For each combination, the best 20 peptides were selected providing a total of 500 peptides, which were then synthesized by solid phase peptide synthesis. Their interactions with C5a-decapeptide

TABLE 2. Bulkiness and charge of amino acid. Bulkiness is represented as volume of amino acid residues (28) and charge is represented by the acidity of amino acid side-chain. (http://en.wikipedia.org/wiki/Amino_acid) Positive value represents basic side-chain, negative value represents acidic side-chain whereas 0 represents natural. Histidine is only weakly basic so it is considered 0 here.

Amino Acid	Residue Volume	Charge
A	88.6	0
R	173.4	1
D	111.1	-1
N	114.1	0
C	108.5	0
E	138.4	-1
Q	143.8	0
G	60.1	0
H	153.2	0
I	166.7	0
L	166.7	0
K	168.6	1
M	162.9	0
F	189.9	0
P	112.7	0
S	89.0	0
T	116.1	0
W	227.8	0
Y	193.6	0
V	140.0	0

were then determined.

Solid-phase peptide synthesis: Peptide synthesis on cellulose membranes.

Membranes were obtained from Intavis (Bergisch Gladbach, Germany). Fluorenylmethyloxycarbonyl (Fmoc) amino acids and N-hydroxybenzotriazole (HOBT) were obtained from Bachem (King of Prussia, PA). N, NV-diisopropylcarbodiimide (DIC) N, NV-dimethylformamide (DMF) and N methylpyrrolidone-2 (NMP), were of the highest available quality and were tested daily for the absence of contaminating free amines by the bromophenol blue method. Fmoc amino acids were preactivated daily by incubating 300 μl of a 0.6 M solution of the Fmoc amino acid with 150 μl of 1.2 M DIC and 150 μl of 1.2 M HOBT (except for Fmoc arginine which has to be preactivated for each coupling). The side chains of the Na Fmoc protected amino acids groups were the following: Pbf (arginine), Trt (asparagine, glutamine, histidine and cysteine), Acm (cysteine), tBu ether (threonine, tyrosine, serine), OtBu ester (aspartic and glutamic acids) Boc (lysine, tryptophan). All solutions were in NMP. An ASP 222 robot (ABIMED) was used for the coupling steps. The standard coupling procedure involved double coupling of a preactivated solution of 0.3 M Fmoc amino acid for 15 min. After coupling, the membrane was treated with DMF (three times, 2 min), and then 10% (vol /vol) acetic anhydride in DMF (10 min, or until decoloration of the spots) was added to block any unreacted amino groups. After piperidine (20% in DMF, vol/vol) deprotection (5 min), the membrane was treated with a 0.005% bromophenol blue solution in DMF (two times, 2 min), washed with methanol (three times, 2 min), and dried using cold air. For the last cycle, deprotection with piperidine was performed before acetylation with 10% acetic anhydride in DMF.

Membrane Probing Protocol-for C5a Peptide.

The peptide array membrane was placed in 20 ml of 100% methanol and shaken for 5 minutes, then washed in 50% methanol/PBS for 5 minutes followed by washing with 20 ml PBS 3 times, each time for 5 minutes. Unspecific binding sites were blocked with 2 % skim milk in PBS-T (PBS/0.2% Tween 20) at room temp for 2 hours or overnight at 4℃. The membrane was then washed once in PBS for 5 minutes. Biotin labeled C5a-decapeptide or Biotin solution (for control) was diluted to a concentration of 50 μg/ml in PBS and incubated with the membranes overnight at 4℃. The membranes were washed 3 times for 5 minutes each with PBS and then incubated for 2 hours with 1 μg/ml Streptavidin-HRP diluted in PBS. The membrane was then washed again three times for 5 minutes each with PBS. Excessive buffer was removed from the membranes by placing white tissue paper on the membrane.

Spots were detected with chemoluminescence detection kit reagents (Chemoluminescence Super Sensitive 2-CHRP substrate Kit BIO-FX 4ml, Piscataway, NJ) after exposure for 60 seconds.

Statistical analysis

C5a binding assay of C-peptides were statistically evaluated with Z score. Z score was calculated using the following formula:

$$Z=\frac{X-\mu}{\sigma}$$

which X is the raw score of each sample, μ is the mean of the population and σ is the standard deviation of the population. The Z score indicates how many standard deviations an observation is above or below the mean. It allows comparison of observations from different control distributions.

RESULTS

Weighting scheme of parameters

Quantitative analysis of the contribution of several physicochemical parameters to the affinity of peptides derived by MIMETIC resulted in depicting mainly three physicochemical parameters. These are the charges of the amino acids, their bulkiness and the hydropathy index. However, the amount contributed by each of these parameters to the overall affinity of c-peptides was difficult to determine in a cut and dry fashion. Consequently to express affinity among c-peptides, we devised a weighting scheme, shown in Table 1, to optimize the quantitative contribution of each term to the affinity.

Using the last C-terminal 10 amino acids (ISHKDMQLGR) of C5a as target, candidate c-peptides were generated by COMPEP according to combinations of the parameter scoring system listed in Table 1. Three physicochemical parameters were included in the scoring system, hydropathy, charge and bulkiness. Weighting of the parameters was assigned to vary the percent contribution of the corresponding parameter to the final score. In this study, weighting of hydropathy was varied from 70% to 100%. Weighting of charge was varied from 0 % to 60% whereas weighting of bulkiness was fixed at 10% due to lack of evidence on how bulkiness relates to protein-protein interaction.

Five hundred candidate c-peptides with best scores were selected and all of the peptides

were synthesized by solid-phased peptide synthesis on an amino group functionalized filter paper. The peptide sheet was incubated with N-terminally biotin-labeled C5a-decapeptide, and binding was detected with horse radish peroxidase (HRP)-labeled streptavidin.

Binding of c-peptides to C5a

As shown in Fig. 1, 13.8% of the candidate peptides exhibited significant binding with C 5a-decapeptide (69 out of 500). Some clusters of sequences showed similar binding, suggesting that candidate peptides generated using the same parameter scoring system possess similar binding affinities towards C5a-decapeptide. The Z scores, densities and amino acid sequences are listed in Table 3. The Z scores represent the standard deviation of sample values relative to control values. We also performed multiple alignments by dividing the c-peptides into three groups. The first group contains c-peptides with Z scores larger than 2.0. The second group and third group include those with Z scores larger than 3.0 and 4.0 respectively. These peptides are aligned using the multiple alignment program ClustalW (8). These 3 groups of alignments demonstrated that sequences of these peptides are notably conserved, especially at the middle region (Fig. 2). Based on all alignment results, the c-peptide sequences from the 3rd to the 7th residues are generally conserved (LALSL), including the last two residues (GI).

As shown in Table 4, all of the designed complementary sequences are heavily weighted for hydropathy (W_1). Complementarity of amino acid charge did not appear to play a significant role since a higher weighting of this parameter caused the designed sequences to interact more weakly with C5a-decapeptide.

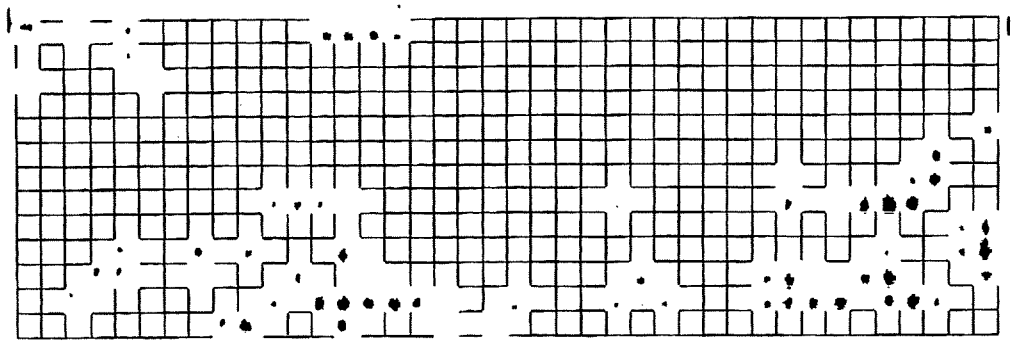

FIG. 1. Membrane of 500 candidate complementary peptides probed with C5a.
Each square represents the area where a candidate complementary peptide was probed with C5a. Black dot indicates that the candidate peptide binds to C5a. The density of a black dot is a reflection of the affinity of the candidate complementary peptide with C5a.

TABLE 3. List of complementary peptides capable of binding with C5a. Their sequences, Z scores, densities and positions on the membrane are listed.

Z	Density	Position	Sequence	Z	Density	Position	Sequence	Z	Density	Position	Sequence
2.649	0.228	1	RAFALTLQTV	5.948	0.482	316	HTIMLTLHGI	0.013	0.024	443	HTLMLTLQSI
0.462	0.059	3	NALALQLNRI	4.592	0.378	317	QTIMLTFHGI	1.197	0.118	451	HALALTIQSI
1.585	0.146	5	QTLMVYFHGI	0.711	0.078	359	RGLVLPLDGI	4.508	0.371	453	QGIAVSLQGV
0.634	0.072	13	RAFAVTLHTV	3.657	0.306	360	RTFLLPLQSI	4.654	0.382	454	QTLALRFQSV
1.62	0.148	14	RAFAISLQRV	0.958	0.097	365	RGLLVPLNGV	3.119	0.264	455	HSLAVSLQTI
2.114	0.186	15	RGFAFRLHTV	4.167	0.345	368	RMLLFSLKGI	4.139	0.343	456	HTFAISLHGI
0.462	0.059	16	QMFMISVNS	2.119	0.187	370	RAFVLWLQSI	1.689	0.154	457	QSVALSLQAI
1.14	0.111	45	HTLALSLQGL	2.697	0.231	374	RGFLLPLRWV	-0.08	0.017	458	QGIAVTLQGV
0.095	0.031	81	QTLDLSLHTI	0.784	0.084	396	HAAVASAQTI	-0.27	0.002	461	QAVALQLQGI
0.572	0.067	86	QTLDLSLHTV	1.757	0.159	399	QALALRLHGI	0.017	0.025	465	HMLALTLHTI
2.11	0.188	200	HGLDLYLHSI	8.4	0.672	400	QALALSLHGI	0.224	0.041	467	QGLALSVQAI
2.731	0.234	238	NSVDLTLQGV	1.06	0.105	404	NGLMLSLHTI	0.202	0.039	471	QMLALTLNSL
0.023	0.025	272	QSFALSLHGL	0.174	0.037	405	QGLALSLHTI	2.786	0.238	472	HRLALTLNTI
0.527	0.064	277	QSFAFTFNTI	0.687	0.076	408	QALALRLQAV	2.849	0.243	473	HSLALTLNTI
3.826	0.319	278	QSFALSLQML	1.949	0.174	412	QALLLSMQGI	2.776	0.238	474	HMLALSIQSI
0.958	0.097	291	HAFALQVHTI	0.325	0.048	415	HAALVTAHGI	4.051	0.336	476	QGLAVSVQAI
1.996	0.177	292	QWALMSLQAV	0.798	0.085	426	QAFAVTVHGI	5.113	0.418	477	HMLALTIQSI
1.251	0.12	293	QALAVHVNSV	0.355	0.051	431	HAFALRLHTV	1.315	0.125	478	QAVALQLQAV
0.605	0.07	294	HRFALYIHAI	2.356	0.205	432	QGFALRLHSV	2.478	0.215	489	QRLELSLNTV
-0.02	0.022	305	QTIMLSLHGI	0.147	0.035	433	NGLALQLQTI	5.71	0.464	490	HALALTLQRV
2.022	0.179	312	HRLALSVHGI	1.878	0.168	435	HAIALTLNGI	3.269	0.276	494	HGFALSLQTL
-0.24	0.005	314	HRLAMTANGI	4.919	0.403	436	QMLALRVHTI	0.109	0.032	498	QAVDLGLHGV
2.267	0.198	315	HTLALGLHGV	3.445	0.289	440	HALALTLQSI	0.157	0.035	500	NRMFIHLQSS

Plotting hydropathies of the 4 complementary sequences of highest Z scores showed a prominent complementary pattern against that of the target region of C5a-decapeptide (Fig. 3). Four peptides of the 471 peptides, which did not bind to C5a-decapeptide, were chosen and their hydropathic profiles were also plotted. These plots were not mirror images of the hydropathic profile of C5a-decapeptide.

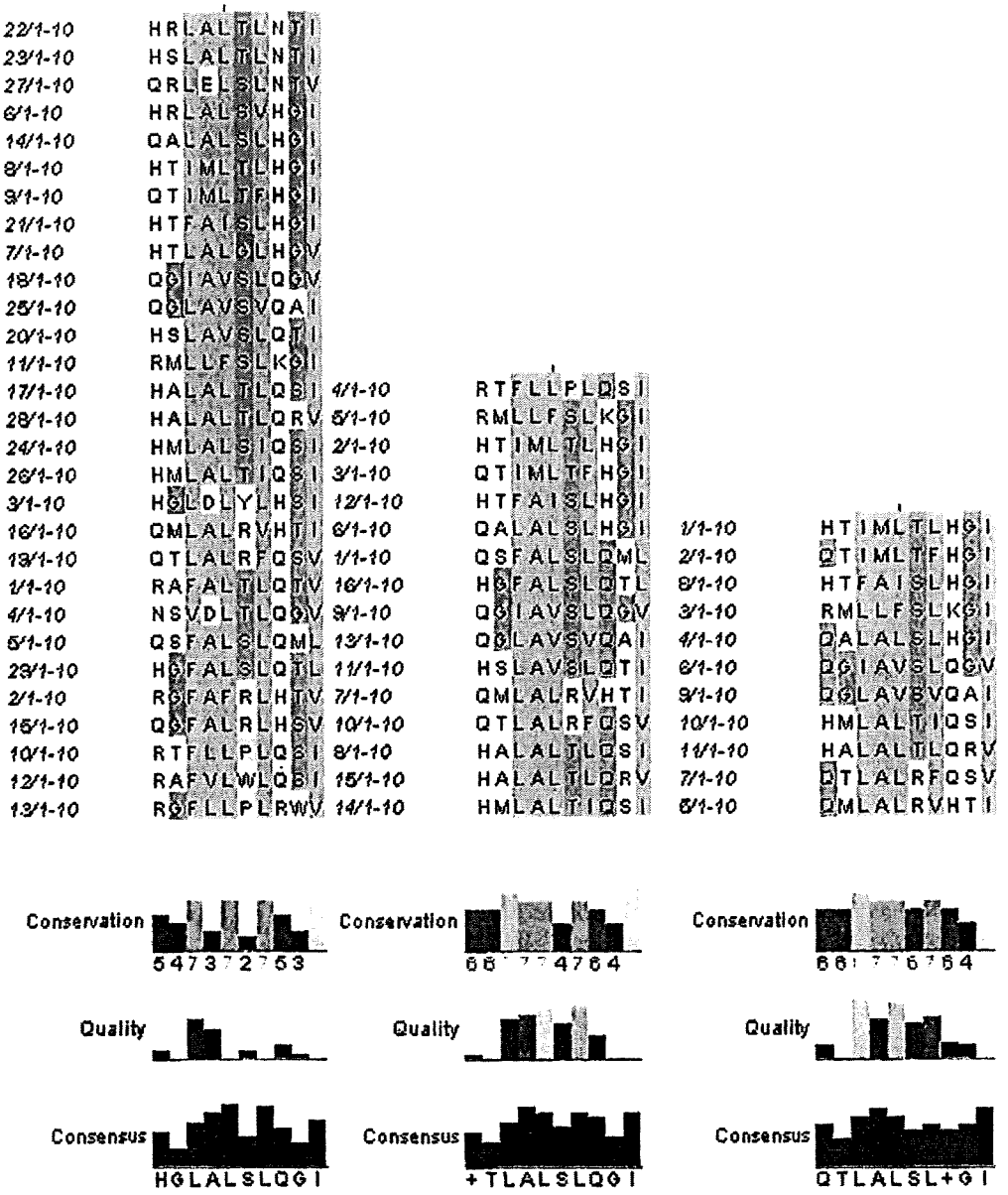

FIG. 2. Multiple alignments of complementary peptides with Z scores using ClustalW. Alignment results are presented here using JalView (9). Left panel: Complementary peptides with Z scores larger than 2. Multiple alignment shows the consensus result as HGLALSLQGI.

Middle panel: Complementary peptides with Z scores larger than 3. Multiple alignment shows the consensus result as +TLALSLQGI.

Right panel: Complementary peptides with Z scores larger than 4. Multiple alignment shows the consensus result as QTLALSL+GI.

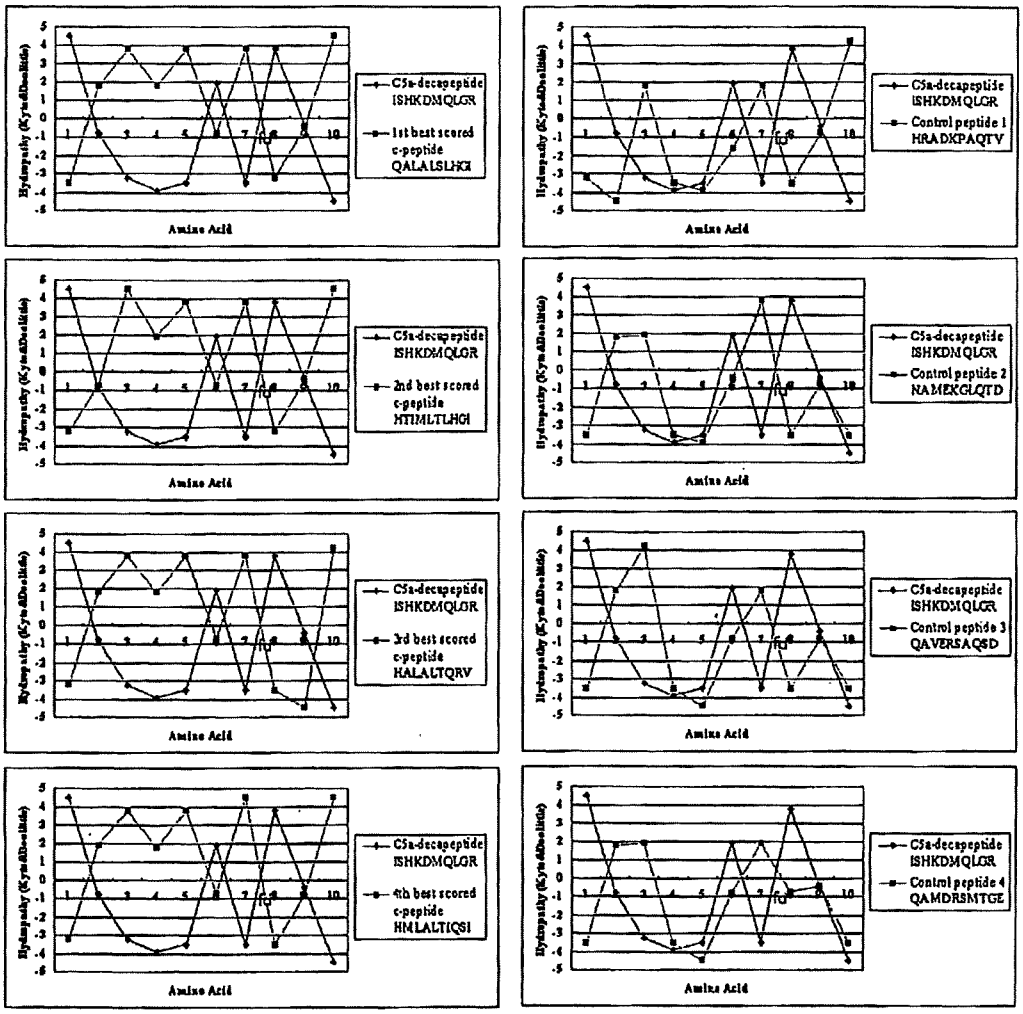

FIG. 3. Hydropathy plots of the 4 complementary peptides with the highest Z scores and 4 peptides without detectable binding affinity (control peptides) against C5a. The Kyte-Doolittle hydropathy scale was adopted (19). Left panel: Sequences of the 4 complementary peptides with highest Z_i scores from 1st to 4th are QALALSLHGI, HTIMLTLHGI, HALALTLQRV and HMLALTIQSI.
Right panel: Of 471 candidate peptides without binding activity to C5a, 4 were selected (control peptides). Their sequences are HRADKPAQTV, NAMEKGLQTD, QAVERSAQSD and QAMDRSMTGE.

DISCUSSION

We have written a computer program COMPEP for designing c-peptides that interact with a target peptide. In this study, designed c-peptides able to bind to the C-terminal of C5a. 69 out of 500 c-peptides exhibited significant interactions with C5a-decapeptide and their charac-

teristics were analyzed. Within different physicochemical parameters used in the program, hydropathy displayed the most significant role, demonstrating that hydropathic complementarity may be a critical parameter for some protein-protein interactions. This result is consistent with many published studies (6, 11-12, 25). The Kyte-Doolittle hydropathy scale was employed since it is widely used in predicting and analyzing secondary structures of proteins (18, 27) and it has also been adopted for analyzing protein-protein interactions in reported results (16, 20). The molecular recognition theory proposed by Markus and Blalock is also based on hydropathic complementarity (20). It states that peptide sequence translated from the antisense strand of a gene is able to interact with the peptide sequence translated from the sense strand due to a tendency that codons of the antisense DNA strand encode amino acids with complementary hydropathy. Rather than designing c-peptides by exploiting the antisense DNA strand to the target sequence, which may not be feasible often due to the presence of a stop codon, in this study we directly incorporated hydropathic complementarity in the calculations. Figure 3 shows that the hydropathy profiles of all 4 highest Z scored peptides displayed mirror images to that of the C5a-decapeptide. Together with the observation that the candidate peptides that reacted strongly with C5a-decapeptide were weighted heavily for hydropathy (Table 4), these results provide remarkable evidence to support the significance of hydropathic complementarity in protein-protein interaction.

TABLE 4. The Z score, density, sequence and weighting of physicochemical parameters of complementary sequences with Z scores larger than 4. W_1, W_2 and W_3 represent weighting for hydropathy, charge and bulkiness.

Z	Density	Position	Sequence	Weighting of parameters (W_1, W_2, W_3)
5.948	0.482	316	HTIMLTLHGI	90,40,10
4.592	0.378	317	QTIMLTFHGI	90,40,10
4.167	0.345	368	RMLLFSLKGI	100,0,0
8.4	0.672	400	QALALSLHGI	100,20,10
4.919	0.403	436	QMLALRVHTI	100,30,10
4.508	0.371	453	QGIAVSLQGV	100,40,10
4.654	0.382	454	QTLALRFQSV	100,40,10
4.139	0.343	456	HTFAISLHGI	100,40,10
4.051	0.336	476	QGLAVSVQAI	100,50,10
5.113	0.418	477	HMLALTIQSI	100,50,10
5.71	0.464	490	HALALTLQRV	100,60,10

Such observation of how C5a-decapeptide preferred those peptides with inverted hydropathic profile to bind with may be decent evidence provided by the nature to support Blalock's theory. As he stated in the molecular recognition theory (5), that the hydropathy of an amino acid is determined by the second base of a codon, and that many evidences have shown that the hydropathic profile of a protein is a key to its gross architecture. Considering that the side-chain of hydrophobic amino acids tend to protrude inwardly to the globular structure, while those of hydrophilic amino acids tend to protrude outward towards the aqueous environment. We can speculate that the structure of, at least for short peptides, a pair of peptides with hydropathic profiles inverted with each other, would have gross structures inverted with each other also. And hence, providing suitable constructs to bind with each other. It is not known for now how much we can exploit this theory to proteins with complex tertiary and quaternary structures. Despite of that, it is undeniable that many peptide antagonists have been successfully designed.

Amino acid charge did not show significant importance for designing complementary peptide in this study. Therefore, overall charge complementarity is probably not necessary to consider in complementary peptide design. However, reports have shown that mutating one or two charged amino acids to ones of opposite charge can interfere with protein-protein interactions (1, 23). We can speculate on this phenomenon due to that the side chain of charged amino acid is relatively bulky, complementary charge effect of one single amino acid at the core of the binding site may enhance the binding infinity if the hindrance of bulkiness of the corresponding amino acids on both sides is trivial.

Multiple alignment of the complementary peptides revealed a fairly consensus outcome. The 3rd to 5th, 7th and last residues displayed a bias towards hydrophobic amino acids whereas slightly hydrophilic amino acids were generally adopted at the 6th residue. This may reflect which positions of complementary peptides are in contact with C5a.

Further investigation of the effect of these designed complementary peptides on C5a biological function and modification of the peptides may afford a new inhibitor of C5a based on targeting the C-terminal. Together with other C5a inhibitors, targeting other regions of C5a may remarkably reduce its effect and hence be suited for treatment of diseases caused by generation of C5a.

Many additional factors may involve in determining whether a peptide can block the biological function of a protein or not. However, to design a peptide able to bind with the target protein is inevitable the crucial step when inventing peptide drugs. This computer program, to-

gether with the solid-phase peptide synthesis and probing, may provide a speedy and inexpensive attempt to achieve it.

ACKNOULEDGEMENT

The authors sincerely thank Dr. Dirk Winkler for his expertise in peptide synthesis and membrane probing.

REFERENCES

1. Absalom NL, Lewis TM, Kaplan W, Pierce KD, Schofield PR. 2003. Role of charged residues in coupling ligand binding and channel activation in the extracellular domain of the glycine receptor. *J. Biol. Chem.* **278** : 50151-50157.
2. Allegretti M, Moriconi A, Beccari AR, Di Bitondo R, Bizzarri C, Bertini R, Colotta F. 2005. Targeting C 5a: recent advances in drug discovery. *Curr. Med. Chem.* **12** : 217-236.
3. Amblard M, Fehrentz JA, Martinez J, Subra G.. 2006. Methods and protocols of modern solid phase Peptide synthesis. *Mol. Biotechnol.* **33** : 239-254.
4. Blalock JE, Smith EM. 1984. Hydropathic anti-complementarity of amino acids based on the genetic code. *Biochem. Biophys. Res. Commun.* **121** : 203-207.
5. Blalock JE. 1995. Genetic origins of protein shape and interaction rules. *Nat. Med.* **1** : 876-878.
6. Brentani RR, Ribeiro SF, Potocnjak P, Pasqualini R, Lopes JD, Nakaie CR. 1998. Characterization of the cellular receptor for fibronectin through a hydropathic complementarity approach. Proc. Natl Acad. Sci. USA **85** : 364-367.
7. Campbell W, Kleiman L, Baranyi L, Li Z, Khorchid A, Fujita E, Okada N, Okada H. 2000. A novel genetic algorithm for designing mimetic peptides that interfere with the function of a target molecule. Microbiol. Immunol. **46** : 211-215.
8. Chenna R, Sugawara H, Koike T, Lopez R, Gibson TJ, Higgins DG, Thompson JD. 2003. Multiple sequence alignment with the Clustal series of programs. *Nucleic Acids Res.* **31** : 3497-3500.
9. Clamp M, Cuff J, Searle SM, Barton GJ. 2004. The Jalview Java Alignment Editor. *Bioinformatics* **20** : 426-427.
10. Ember JA, Hugli TE. 1997. Complement factors and their receptors. *Immunopharmacology* **38** : 3-15.
11. Fassina G, Cassani G. 1992. Design and recognition properties of a hydropathically complementary peptide to human interleukin 1 beta. *Biochem. J.* **282** : 773-779.
12. Fassina G, Melli M. 1994. Identification of interactive sites of proteins and protein receptors by computer-assisted searches for complementary peptide sequences. *Immunomethods* **5** : 114-120.
13. Fujita E, Farkas I, Campbell W, Baranyi L, Okada H, Okada N. 2004. Inactivation of C5a anaphylatoxin by a peptide that is complementary to a region of C5a. J. Immunol. **172** : 6382-6387.
14. Gerard C, Gerard NP. 1994. C5a anaphylatoxin and its seven transmembrane-segment receptor. *Annu.*

Rev. Immunol. 12 : 775-808.

15. Guo RF, Riedemann NC, Ward PA. 2004. Role of C5a-C5aR interaction in sepsis. *Shock* 21 : 1-7.
16. Heal JR, Bino S, Ray KP, Christie G, Miller AD, Raynes JG. 1999. A search within the IL-1 type I receptor reveals a peptide with hydropathic complementarity to the IL-1 beta trigger loop which binds to IL -1 and inhibits in vitro responses. *Mol. Immunol.* 36 : 1141-1148.
17. Huber-Lang MS, Sarma JV, McGuire SR, Lu KT, Padgaonkar VA, Younkin EM, Guo RF, Weber CH, Zuiderweg ER, Zetoune FS, Ward PA. 2003. Structure-function relationships of human C5a and C5aR. *J. Immuno.* 170 : 6115-6124.
18. Klevanik AV. 2001. Hydrophobicity and prediction of the secondary structure of membrane proteins and peptides. *Membr. Cell Biol.* 14 : 673-697.
19. Kyte K, Doolittle RF. 1982. A simple method for displaying the hydropathic character of a protein. *J. Mol. Biol.* 157 : 105-132.
20. Markus G, Tritsch GL, Parthasarathy R. 1989. A model for hydropathy-based peptide interactions. *Arch. Biochem. Biophys.* 272 : 433-439.
21. Mitchell M. 1996. An Introduction to Genetic Algorithms. MIT Press, Cambridge, MA.
22. Mollison KW, Mandecki W, Zuiderweg ER, Fayer L, Fey TA, Krause RA, Conway RG, Miller L, Edalji RP, Shallcross MA, et al. 1989. Identification of receptor-binding residues in the inflammatory complement protein C5a by site-directed mutagenesis. *Proc. Natl. Acad. Sci. USA* 86 : 292-296.
23. Nassar N, Horn G, Herrmann C, Block C, Janknecht R, Wittinghofer A. 1996. Ras/Rap effector specificity determined by charge reversal. *Nat. Struct. Biol.* 3 : 723-729.
24. Okada N, Asai S, Hotta A, Miura N, Ohno N, Farkas I, Hau L, Okada H. 2007. Increased inhibitory capacity of an anti-C5a complementary peptide following acetylation of N-terminal alanine. *Microbiol. Immunol.* 51 : 439-443.
25. Pasqualini R., Chamone DF, Brentani RR. 1989. Determination of the putative binding site for fibronectin on platelet glycoprotein IIb-IIIa complex through a hydropathic complementarity approach. *J. Biol. Chem.* 264 : 14566-14570.
26. Shimomura Y, Kawamura T, Komura H, Campbell W, Okada N, Okada H. 2003. Modulation of procarboxypeptidase R (ProCPR) activation by complementary peptides to thrombomodulin. *Microbiol. Immunol.* 47 : 241-245.
27. Suarez T, Gallaher WR, Agirre A, Goni FM, Nieva JL. 2000. Membrane interface-interacting sequences within the ectodomain of the human immunodeficiency virus type 1 envelope glycoprotein: putative role during viral fusion. *J. Virol.* 74 : 8038-8047.
28. Zamyatin AA. 1972. Protein Volume in Solution. *Prog. Biophys. Mol. Biol.* 24 : 107-123.
29. Zuiderweg ER, Nettesheim DG, Mollison KW, Carter GW. 1989. Tertiary structure of human complement component C5a in solution from nuclear magnetic resonance data. *Biochemistry* 28 : 172-85.

Available online at www.sciencedirect.com

ScienceDirect

Neurochemistry International 52 (2008) 846–856

NEUROCHEMISTRY International

www.elsevier.com/locate/neuint

Estrogen enhances expression of the complement C5a receptor and the C5a-agonist evoked calcium influx in hormone secreting neurons of the hypothalamus

Imre Farkas [a,*], Patricia Varju [a], Emese Szabo [a], Erik Hrabovszky [a], Noriko Okada [b], Hidechika Okada [c], Zsolt Liposits [a,d]

[a] *Laboratory of Endocrine Neurobiology, Institute of Experimental Medicine, Hungarian Academy of Sciences, Szigony u. 43, 1083 Budapest, Hungary*
[b] *Department of Biodefense Medicine, Nagoya City University Graduate School of Medical Sciences, Nagoya, Aichi 467-8601, Japan*
[c] *Choju Medical Institute, Fukushimura Hospital, Toyohashi, Aichi 441-8124, Japan*
[d] *Department of Neuroscience, Information Technology Faculty, Péter Pázmány Catholic University, Budapest, Hungary*

Received 3 August 2007; received in revised form 17 September 2007; accepted 24 September 2007
Available online 29 September 2007

Abstract

In the present study we examined presence of the complement C5a receptor (C5aR) in hypothalamic neurosecretory neurons of the rodent brain and effect of estrogen on C5aR expression. Whole cell patch clamp measurements revealed that magnocellular neurons in the supraoptic and paraventricular nuclei of hypothalamic slices of the rats responded to the C5aR-agonist PL37-MAP peptide with calcium ion current pulses. Gonadotropin-releasing hormone (GnRH) producing neurons in slices of the preoptic area of the mice also reacted to the peptide treatment with inward calcium current. PL37-MAP was able to evoke the inward ion current of GnRH neurons in slices from ovariectomized animals. The amplitude of the inward pulses became higher in slices obtained from 17β-estradiol (E2) substituted mice. Calcium imaging experiments demonstrated that PL37-MAP increased the intracellular calcium content in the culture of the GnRH-producing GT1-7 cell line in a concentration-dependent manner. Calcium imaging also showed that E2 pretreatment elevated the PL37-MAP evoked increase of the intracellular calcium content in the GT1-7 cells. The estrogen receptor blocker Faslodex in the medium prevented the E2-evoked increase of the PL37-MAP-triggered elevation of the intracellular calcium content in the GT1-7 cells demonstrating that the effect of E2 might be related to the presence of estrogen receptor. Real-time PCR experiments revealed that E2 increased the expression of C5aR mRNA in GT1-7 neurons, suggesting that an increased C5aR synthesis could be involved in the estrogenic modulation of calcium response.

These data indicate that hypothalamic neuroendocrine neurons can integrate immune and neuroendocrine functions. Our results may serve a better understanding of the inflammatory and neurodegeneratory diseases of the hypothalamus and the related neuroendocrine and autonomic compensatory responses.

Keywords: Hypothalamus; Complement C5a receptor; Neurosecretory neurons; Estrogen

1. Introduction

Multidirectional communication exists between the neuroendocrine and immune systems. Inflammation, for example, suppresses pulsatile gonadotropin-releasing hormone (GnRH) secretion resulting in disruption of the ovarian cycle and fertility (Karsch et al., 2002). Reversely, endocrine hormones also affect functions of the classical immune organs. In addition to its known effects modulating, for example, the electric and endocrine functions of neuroendocrine cells (Farkas et al., 2007; Thakur and Sharma, 2007), estrogen increases the levels of inducible nitric oxide synthase, nitric oxide and interferon-γ in splenocytes (Karpuzoglu and Ahmed, 2006). However, very little is known about the mechanism whereby hormones of endocrine glands modulate immune responses in the brain.

The central nervous system (CNS) utilizes its own protection systems including the complement system (C) to eliminate invading microorganisms. Numerous cell types, such as

* Corresponding author. Tel.: +36 1 210 9400x368; fax: +36 1 210 9944.
E-mail address: farkas@koki.hu (I. Farkas).

0197-0186/$ – see front matter © 2007 Elsevier Ltd. All rights reserved.
doi:10.1016/j.neuint.2007.09.014

neurons, endothelial cells, astrocytes, microglia and oligodendrocytes (Thomas et al., 2000; Gasque et al., 2000) have been identified as sources of complete and functional C in the brain. In addition, expression of various components of C has also been detected in affected neurons of Alzheimer's disease (AD) patients (Shen et al., 1997; Terai et al., 1997; Strohmeyer et al., 2000). Anaphylatoxins including C5a, that can be generated during activation of C, have also been identified in the brain. C5a is a 74 amino acid-long peptide, which is cleaved from the C5 component of C during inflammation (Rother et al., 1998). Binding of C5a to its receptor (C5aR) evokes several responses such as increased intracellular calcium content, phagocytosis, chemotaxis, degranulation and the synthesis and release of various inflammatory mediators (Konteatis et al., 1994; Rother et al., 1998). Expression of C5aR has been revealed in astrocytes and microglia of the CNS (Gasque et al., 1995, 1997). Neurons of the hippocampal formation, pyramidal cells of the cerebral cortex, Purkinje cells in the cerebellum and a subset of thalamic neurons equally synthesize this receptor in rodents (Stahel et al., 1997a,b; VanBeek et al., 2000). Likewise, C5aR has been revealed in human hippocampal and cortical pyramidal neurons and neuroblastoma cells (Farkas et al., 1998b, 1999, 2003; O'Barr et al., 2001). In contrast, only limited information is available about the expression and role of C5aR in the hypothalamus, the main central regulator of neuroendocrine axes and autonomic functions. The axonal processes of the hypophysiotrophic parvicellular neurons and also those of the magnocellular neurosecretory cells terminate outside the blood–brain barrier, in the median eminence and the posterior pituitary, respectively. Therefore, these neuroendocrine cells occupy an ideal anatomical position to sense and mediate the peripheral immune signals to various endocrine axes.

While the anti-inflammatory and neuroprotective effects of estrogen are well established (Kovacs, 2005; Suzuki et al., 2006; Turgeon et al., 2004) recent studies have demonstrated that this hormone plays a rather complex role in the immune response of the brain (Sohrabji, 2005; Morale et al., 2006). Compelling evidence has been provided to prove that estrogen is required for a proper immune response in the CNS (Soucy et al., 2005) including the hypothalamus that is known to control the neuroendocrine axes and the autonomic nervous system. In the present study we addressed the issue of whether neuroendocrine cells synthesize functional C5aR. Whole cell clamp electrophysiology, real-time PCR and calcium imaging were used to examine the effects of C5aR activation upon various hypothalamic neurosecretory cells, such as magnocellular neurons and GnRH-producing neurons. In addition, the modulatory effect of estrogen was studied on the response triggered by activation of C5aR in hypothalamic neurons.

2. Methods

2.1. Experimental animals and cell line

Rats and mice were housed in light- and temperature controlled environment with free access to food and water and treated in accordance with the legal requirements of the Animal Care and Use Committee of the Institute of Experimental Medicine and the European Community (Decree 86/609/EEC). All experimental protocols were reviewed and approved by the Animal Welfare Committee at the Institute of Experimental Medicine. All efforts were made to minimize animal suffering and the number of animals used.

Magnocellular neurons of the paraventricular (PVN) and supraoptic (SON) nuclei and GnRH-producing cells of the preoptic area were chosen as model systems to examine the effects of C5aR activation on neuroendocrine cells. Magnocellular neurons of the PVN and SON could be easily visualized in the rat brain slice by their characteristic location, shape and size. The immortalized GT1-7 neuronal cell line which produces GnRH was generated and kindly provided for these studies by Dr. Pamela L. Mellon (Mellon et al., 1990). In order to visualize GnRH neurons in the brain slices, GnRH-enhanced green fluorescent protein (GnRH-GFP) transgenic mice (kind gift by Dr. Suzanne Moenter) were chosen in which the GnRH promoter drives selective GFP expression in the majority of GnRH neurons (Suter et al., 2000).

2.2. Estrogen treatment paradigms

Six adult female GnRH-GFP mice at the age of 100 days were ovariectomized (OVX) bilaterally under pentobarbital anesthesia (35 mg/kg bw, i.p.) and allowed to survive for 1 week to decrease endogenous sex steroid levels. Then three of them (OVX group) received a single subcutaneous (s.c.; 100 μl) injection of sunflower oil vehicle. The other three mice (OVX + E2 group) were injected s.c. with 17β-estradiol (E2; 2 ng/g body weight) in vehicle. This dose of estradiol was chosen because a saturating dose of estradiol is approx. 3.6 ng/g bodyweight (BW) in rats (Brown et al., 1992). Applying the 2 ng/g subsaturating dose we could avoid pharmacological responses due to supraphysiological estradiol levels.

The animals were sacrificed 24 h after receiving injection. Brain slices were then prepared for the electrophysiological recording.

2.3. C5aR-agonist peptide (PL37-MAP)

The amino acid sequence (RAARISLGPRCIKAFTE) of the C5aR-agonist peptide (PL37-MAP) is a fragment of C5a and represents antisense-homology-box (AHB) region of C5a (Baranyi et al., 1995, 1996). The peptide was synthesized in multiple antigenic peptide (MAP) form.

The main reason to choose PL37-MAP instead of C5a was the carboxypeptidase activity existing in the brain slice (Che et al., 2005). Carboxypeptidase removes Arg from the C-terminal of C5a, therefore, the effective concentration of the intact C5a changes quickly. In addition, due to the carboxypeptidase activity, two active forms of C5a (the intact C5a and the desArg-C5a, both of them having different effect when activating the C5aR) would exist simultaneously in the brain slice during the experiment. The unpredictably changing ratio of the two forms would make the sound measurement difficult. We could avoid this difficulty by using the C5aR-agonist PL37-MAP.

During the experiments the PL37-MAP peptide was pipetted directly into the bath fluid of the cells to be recorded.

2.4. Cell culture

GT1-7 cells were cultured in Dulbecco Modified Eagle Medium (DMEM) containing high-glucose and supplemented with 10% fetal calf serum (FCS) and 5% horse serum (HS). Before estrogen treatment the culturing medium was replaced with a steroid/thyroid- and phenol red-free one and cells were cultured in this medium for 48 h. Subsequently, the cells were treated with water-soluble E2 (SIGMA) at 20 nM and then used at various time points in PCR ("t" = 0.5, 2, 8, 24 and 48 h) and calcium imaging experiments (24 h). The control cells were used after the steroid-withdrawal period of 48 + "t" hours. In order to determine if estrogen receptor was involved in the observed effects, other control cells were co-treated with E2 and the estrogen receptor blocker Faslodex (ICI 182,780; 1 μM; Tocris Inc.).

2.5. Reverse transcription

Total RNA samples from control and E2 treated GT1-7 cells were isolated with TRIzol LS reagent (Invitrogen) according to the manufacturers instructions.

RNA from three equivalent cultures were mixed and the RNA solutions were diluted to reach a final concentration of 1 μg/μl. From each treatment group 2 μg total RNA was used for cDNA synthesis. cDNA reaction mixtures (40 μl) contained oligodT, random hexamers and 1.5 mM $MgCl_2$. Reverse transcription was performed in a Perkin-Elmer thermal cycler with the ImProm II Reverse Transcription System (Promega) according to instructions by the manufacturer.

2.6. Real-time quantitative PCR

Real-time polymerase chain reactions (PCR) were carried out in a Light Cycler PCR machine (Roche) with the DNA Master SYBR Green I mix (Roche) following the manufacturer's protocols. Each RT-PCR experiment was performed in triplicate. The 10 μl reaction volumes were placed in Light Cycler glass capillaries (Roche) and composed of 1 μl DNA Master SYBR Green I (Roche), 1 μl cDNA mix, 4 mM $MgCl_2$ and 0.3 μM specific primers. The transcript of the house keeping gene hypoxanthine-guanine phosphoribosil transferase (HPRT), which is not regulated by estrogen, was used as an internal control to compensate for variations in amplification efficiency when the amounts of the C5aR amplicon were calculated.

The standard curves were created by amplifications of oligonucleotides containing partial sequences of the HPRT and C5aR genes with the same primer sequences as used for the amplification of experimental samples. The oligonucleotide standards were prepared using serial 1:10 dilutions with TE buffer, over a concentration range spanning the sample concentrations. For quantification, the test oligonucleotide was used at a dilution close to the sample concentrations and the reverse transcribed RNA isolated at 0, 0.5, 2, 8, 24 and 48 h after estrogen treatment. H_2O was included as no template control. Real-time PCR conditions were as follows: HPRT: 95 °C, 5 min for denaturation; 65 cycles: 94 °C, 5 s; 57 °C, 7 s; 72 °C, 10 s; C5aR: 95 °C, 5 min; 65 cycles for 94 °C, 5 s; 57 °C, 7 s and 72 °C, 10 s and cooling to 40 °C, 30 s. Primer sequences used in the PCR reactions were as follows: HPRT forward 5′-tgt aat gat cag tca acg ggg-3′, reverse 5′-tgg cct gta tcc aac act tcg-3′; the C5aR primer was 5′-tgc cct ggt ggt gtg ggt ga-3′ (forward) and 5′-agg acg gaa tgg tga gga gc-3′ (reverse).

The relative amount of the products was determined from the log phase of the reaction.

2.7. Calcium imaging

Cultured GT1-7 cells were loaded with the calcium-sensitive fluorescent dye Fura-2 AM (1 μM; Molecular Probes, Eugene, OR, USA) in loading buffer containing 0.1% DMSO (Molecular Probes) in 1.5 h at room temperature (RT). After washing with Hanks' Balanced Salt Solution (HBSS), the experiments were carried out at RT. The PL37-MAP peptide (62.5–250 nM) was pipetted directly onto the cells in HBSS after a 4 min baseline recording and then the diluted peptide remained in the HBSS during recording. In the case of E2 pretreatment, the cells were pretreated with E2 as described in Section 2.4 and all of the rinsing and extracellular solutions contained the same concentration of E2. After the 4 min baseline recording the PL37-MAP peptide (62.5–125 nM) was introduced into the bath fluid containing E2 and then the diluted peptide remained in the HBSS–E2 mixture during recording.

The experiments were carried out with a Deltascan Model 4000 calcium imaging system (Photon Technology International, Princeton, NJ, USA), using the ratio of the fluorescent signals obtained at excitation wavelengths of 340 and 380 nm to determine changes in the intracellular calcium concentration.

2.8. Brain slice preparation

Animals (22 ± 5-day-old male Wistar rats for recording in the SON, PVN and anterior hypothalamic area [AHA] and 110 ± 12-day-old female mice for recording GnRH-GFP neurons) were anaesthetized with pentobarbital (35 mg/kg bw, i.p.) and decapitated. The brains were removed, and then immersed in ice cold artificial cerebrospinal fluid (ACSF; NaCl 140 mM, KCl 3 mM, $MgSO_4$ 1.3 mM, NaH_2PO_4 1.4 mM, $CaCl_2$ 2.4 mM, glucose 11 mM, HEPES 5 mM, pH 7.25) bubbled with 95% O_2–5% CO_2. Hypothalamic blocks were dissected from the rat and mouse brains and 300 μm thick slices containing the PVN, SON and AHA of rats or GnRH neurons in the preoptic area of mice, were sectioned with a VT-1000S vibratome (Leica GmBH, Germany) using a sapphire knife (Delaware Diamond Knives Inc., Wilmington, DE, USA) in ice cold and oxygenated ACSF. The slices were bisected along the third ventricle and equilibrated in ACSF saturated with O_2/CO_2 mixture at RT for 1.5 h. In order to record the neurons, the equilibrated hemi-slices were placed in an immersion-type recording chamber.

2.9. Whole cell clamp experiments

The cells were voltage clamped at RT using a whole cell clamp configuration. The instruments used for electrophysiology were as follows: Axopatch 200B patch clamp amplifier, Digidata-1322A data acquisition system and pCLAMP 9.2 software (Axon Instruments-Molecular Devices Co., Sunnyvale, CA, USA), the headstage of the amplifier was fitted to a MHW-3 hydraulic micromanipulator (Narishige Co., Japan). The cells were visualized by a BX51WI upright microscope (Olympus Co., Japan) equipped with an epifluorescent filter set (excitation filter: U-HQ450–490; dichroic mirror U-Q495LP; emission filter: U-HQ490–540) capable of visualizing the GnRH-GFP neurons in the brain slice and a Cohu 4912 CCD camera (Cohu Inc., San Diego, CA, USA) driven by a Scion Image for Windows Beta 4.0.2 software (Scion Co., Frederick, MD, USA). The microscope and the micromanipulator were fitted to a S'Table antivibration table equipped with a Petra platform (Supertech Co., Hungary-Switzerland). Softwares were run on an IBM compatible personal computer. The patch electrodes (o.d. = 1.5 mm, thin wall, Garner Co., USA) were pulled with a Flaming-Brown P-97 horizontal puller (Sutter Instrument Co., Novato, CA, USA) and polished with an MF-830 microforge (Narishige). Resistance of patch electrodes was 8–10 MΩ for GT1-7 cells and 2–3 MΩ for the neurons in the brain slices.

The solutions for electrophysiological recording were as follows: extracellular solution for GT1-7 cells (HEPES 10 mM, NaCl 140 mM, KCl 5 mM, $CaCl_2$ 2 mM, $MgCl_2$ 2 mM, glucose 10 mM, pH 7.34) and ACSF for brain slices (see Section 2.8 for composition of ACSF); intracellular pipette solution (HEPES 10 mM, KCl 110 mM, NaCl 15 mM, $CaCl_2$ 0.1 mM, $MgCl_2$ 2 mM, EGTA 1 mM, pH 7.25). The brain slices were oxygenated by bubbling the extracellular solution with O_2/CO_2 gas mixture during recording at RT.

Using the epifluorescent filter set, GnRH-GFP neurons were identified in the acute brain slices by their green fluorescence, typical fusiform shape and apparent topographic location in the preoptic area.

Holding potential was −50 mV at the GT1-7 cells and −70 mV at the neurons in the brain slices. Pipette offset potential, series resistance and capacitance were compensated before recording. Only cells with low leakage were used for electrophysiological measurements. The cells requiring any leak subtraction were omitted.

Electrophysiological recordings started simultaneously with the peptide treatment.

Complement C5a (5 μg/ml, human recombinant; Sigma) treatment was carried out by adding C5a to the extracellular solution. The cells were exposed to C5a for 10 min before the patch clamp recording.

$CoCl_2$ was added to the bath solution at 0.5 mM.

2.10. Statistical analyses

Data are presented as mean ± S.E.M.

Statistical analyses (one-way parametric ANOVA and Newman–Keuls multiple comparison test) of the calcium imaging measurements were carried out on $n \geq 14$ cells at each recording using a Prism software package (GraphPad Software, San Diego, CA, USA). Integration and determining maximum of the recorded curves were carried out after subtractive baseline correction.

Electrophysiological recordings were carried out on at least eight cells for each experiment. The average of maximum values of the recorded ion currents was calculated using the PClamp 9.2 software then Student's *t*-test of the Prism software was applied to perform the statistical analysis.

3. Results

3.1. Calcium imaging

Experiments showed that extracellularly applied C5aR-agonist PL37-MAP peptide evoked elevation in the intracellular

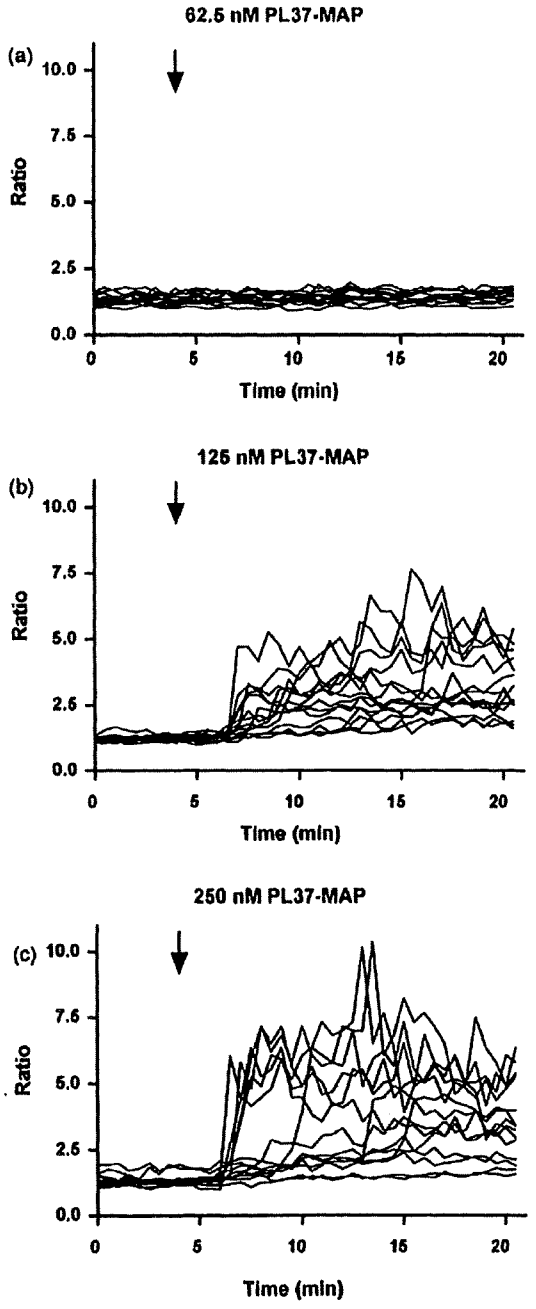

Fig. 1. Calcium imaging measurements of the GT1-7 cells upon treatment with various concentration of the C5a-agonist PL37-MAP peptide. Application of the peptide is shown with arrow. Low concentration of the peptide (62.5 nM) (a) failed to evoke calcium influx. Higher concentrations of PL37-MAP (125 nM) (b) and 250 nM (c) triggered significant elevation of the intracellular calcium content. "Ratio" (vertical axis) refers to the ratio of the fluorescent signals obtained at excitation wavelengths of 340 and 380 nm to determine changes in the intracellular calcium concentration.

calcium content in the fura 2-AM loaded neurons of the gonadotropin-releasing hormone (GnRH) producing GT1-7 cell line (Fig. 1a–c). The peptide did not elevate the calcium content at 62.5 nM (Fig. 1a) whereas change could be recorded at higher concentration of PL37-MAP (125 and 250 nM) (Fig. 1b and c). Elevation started within 2–5 min after introducing the peptide into the bath fluid. Peak amplitude of the ratio value increased with increasing concentration of the PL37-MAP added. After baseline correction, the average maximum peak amplitude of the ratio value was 0.2 ± 0.03 ($n = 14$) at 62.5 nM peptide, 2.35 ± 0.24 ($n = 17$) at 125 nM peptide and 4.55 ± 0.8 ($n = 17$) at 250 nM peptide (Fig. 2a), showing significant increase in the calcium signal (ANOVA: $p < 0.0001$ and $F = 19.26$; Newman–Keuls: $p < 0.01$ for each comparison). The integrated area of the recorded curves representing the net changes in the intracellular free calcium content also revealed significant increase in the calcium signal (Fig. 2b) (ANOVA: $p < 0.0001$ and $F = 179.3$; Newman–Keuls: $p < 0.001$ for each comparison).

In order to examine whether estrogen interacted with the calcium signal mediated via the C5aR, the GT1-7 cells were pretreated with E2 (20 nM) then effect of the PL37-MAP was recorded (Fig. 3a–d) at two concentrations of the peptide (62.5 and 125 nM). In contrast to the result shown in Fig. 1a, at 62.5 nM the peptide elevated the intracellular calcium concentration if the cells were pretreated with E2 (Fig. 3a) showing that E2 potentiated the C5aR-related response of the cells. Similarly, when 125 nM PL37-MAP was applied, E2 increased the calcium influx (Fig. 3c). In order to demonstrate that the effect of E2 could be mediated via estrogen receptor, E2 was co-administered with the estrogen receptor blocker Faslodex (1 μM). Under this condition the response of the cells to 62.5 and 125 nM PL37-MAP did not differ from the calcium signal recorded without E2 showing that Faslodex inhibited the potentiating effect of E2 (Fig. 3b and d). Faslodex alone did not affect the response and the recorded curve was similar to the one measured without E2 (not shown). After baseline subtraction, the average maximum of the recorded curves was 3.8 ± 0.9 (125 nM PL37-MAP + E2; $n = 18$; Newman–Keuls test comparing with the control: $p < 0.05$), 3.5 ± 1.2 (62.5 nM PL37-MAP + E2; $n = 15$; Newman–Keuls test comparing with the control: $p < 0.01$), 2.0 ± 0.4 (125 nM PL37-MAP + E2 + Faslodex; $n = 15$; Newman–Keuls test comparing with the control: $p > 0.05$) and 0.3 ± 0.06 (62.5 nM PL37-MAP + E2 + Faslodex; $n = 14$; Newman–Keuls test comparing with the control: $p > 0.05$), showing that E2 significantly increased the average maximum amplitude (ANOVA for 125 nM PL37-MAP: $p = 0.0098$ and $F = 4.196$; for 62.5 nM: $p = 0.0065$ and $F = 4.571$) and that effect of E2 was abolished by Faslodex (Fig. 4a and c). The normalized areas-under-curve representing the net changes in the intracellular free calcium content also showed significant increase when PL37-MAP was administered to GT1-7 cells pretreated with E2 in the absence of Faslodex (Fig. 4b and d). Increase in the calcium signal of the E2-pretreated cells started in 2–5 min after applying the peptide. The time to start did not differ significantly from the curves recorded without E2.

3.2. Whole cell clamp measurements

Electrophysiology provided further evidence that hypothalamic neurons express functional C5aR and estrogen interacts with the signal activated by the C5a. Whole cell clamp

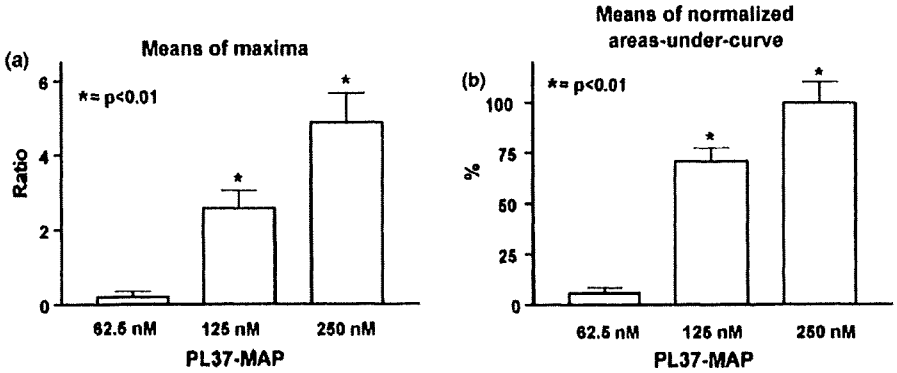

Fig. 2. Histograms of the data recorded in Fig. 1. Maximal amplitude of the curves shows significant ($p < 0.01$) concentration-dependent elevation (a). The areas-under-curve representing the net calcium influx also demonstrates significant ($p < 0.01$) concentration-dependent increase in the calcium content (b). Both histograms were calculated after baseline subtraction. The areas-under-curve data were then normalized by setting the calculated data recorded at application of 250 nM peptide as 100%. The mean ± S.E.M. values of the "means of maxima" were calculated by first determining the maximum amplitude of calcium recording of each cell within the same treatment. Then the calculation of the mean and the S.E.M. was carried out.

measurements demonstrated that 250 nM PL37-MAP evoked inward ion current pulses in GT1-7 cells (Fig. 5a). Amplitude of the pulses was 304 ± 69 pA ($n = 12$). Magnocellular neurons of the supraoptic (SON) and paraventricular (PVN) nuclei of rat brain slices also responded with inward current pulses (SON: 1043 ± 129 pA, $n = 9$; PVN: 1467 ± 219 pA, $n = 10$) to the PL37-MAP (2 μM) administration (Fig. 5b and c). Response of GT1-7 cells to the peptide treatment suggested that GnRH neurons in the brain slice might also react to the PL37-MAP. Therefore, GnRH-GFP neurons of the mice were also treated with PL37-MAP (2 μM) and, indeed, the peptide could trigger inward current pulses in these cells (580 ± 82 pA; $n = 8$; Fig. 5d). In contrast, non-neuroendocrine neurons of the anterior hypothalamic area (AHA; $n = 8$) did not respond to the PL37-MAP administration (Fig. 5e) suggesting that these cells do not possess C5aR in their membrane. After 5 min PL37-MAP treatment the peptide was washed out and 28% of the cells recovered, whereas in the other neurons the inward current

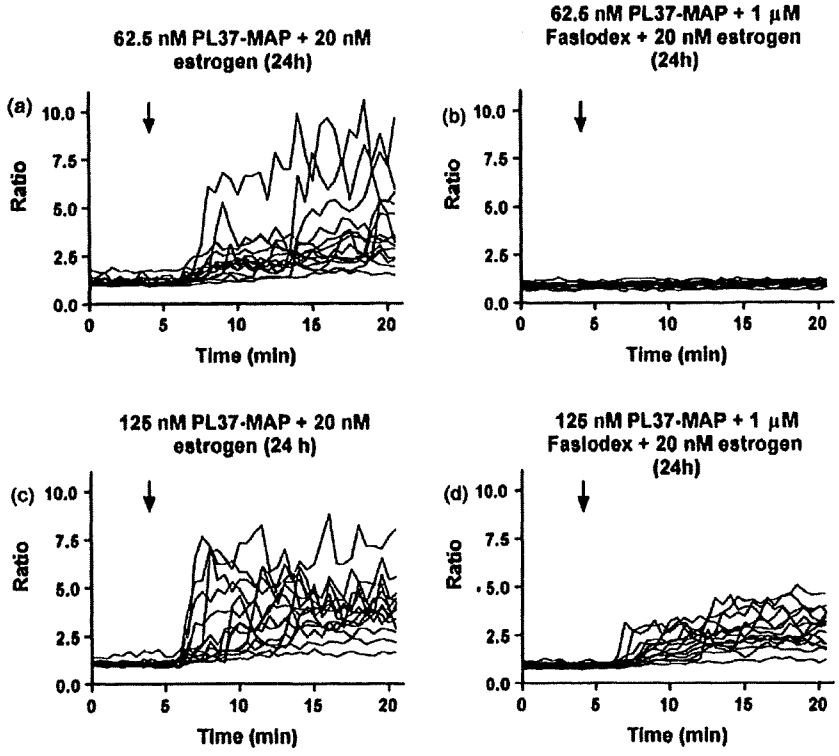

Fig. 3. Calcium imaging measurements of GT1-7 cells pretreated with E2 and then treated with two concentrations of the PL37-MAP. When the cells were pretreated with E2, even low concentration of the peptide (62.5 nM) evoked calcium influx (a). Higher concentration of the peptide (125 nM) also elicited calcium influx (c). However, when E2 was co-applied with the estrogen receptor blocker Faslodex, response of the cells was eliminated at low concentration of PL37-MAP (b) and was attenuated at 125 nM peptide (d). Arrow shows application of the peptide.

話題

相補性ペプチドによる炎症の制御

今井優樹[1)]/岡田則子[2)]

(KEYWORDS)　相補性ペプチド，アナフィラトキシンC5a，炎症

1. はじめに

生物は，細菌やウイルスなどの微生物の体内への感染・侵入に対して，補体やToll-like receptor(TLR)に代表される自然免疫系の生体内防御機構を活性化させ，それらを体内からすばやく排除する仕組みを備えている．自然免疫がひとたび病原体の感染を感知すると，免疫応答に必須な炎症性サイトカインが産生され，生体内で炎症反応を引き起こし，免疫系にかかわる細胞を，感染局所に動員して病原体を排除する．しかし一方で，これらの防御反応の異常亢進により，アレルギーや自己免疫疾患が誘発されたり，重症化した場合には敗血症，播種性血管内凝固症候群(disseminated intravascular coagulation；DIC)，多臓器不全(multiple organ failure；MOF)などの全身性炎症反応症候群(systemic inflammatory response syndrome；SIRS)病態へと進展する．現在まで，様々な敗血症の動物実験モデルが作られ，またいくつもの薬剤の臨床試験が行われてきたが，いまだに臨床の場における敗血症などの過剰な炎症反応に起因する致死的病態を改善する薬剤は登場していない．

本稿では過剰な炎症反応を制御することを目的に創出された相補性ペプチド(complementary peptide)について概説するとともに，相補性ペプチドの今後の可能性について述べる．

2. 相補性ペプチド

ポリペプチド鎖から構成される蛋白質では，分子内でアミノ酸配列自身が情報化され，分子内にセンスペプチド・アンチセンスペプチドの関係によって，相互に対応する配列情報をもつ部分が散在することが，1995年Baranyiらにより見いだされ[1)]，この部分をアンチセンスホモロジーボックス(antisense homology box；AHB)と命名した．アンチセンスペプチドはその特徴としてセン

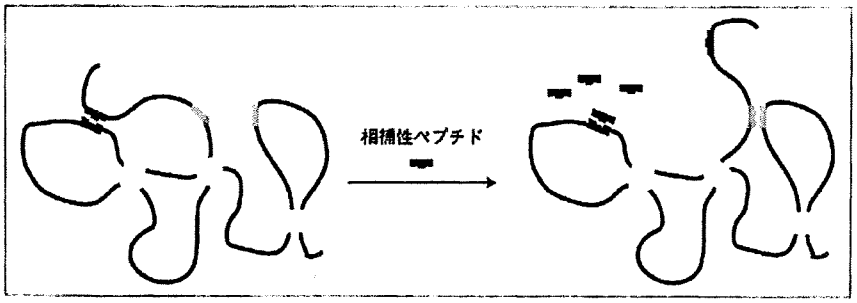

図1　AHBペプチドによる標的蛋白質分子の機能制御

1) IMAI Masaki　名古屋市立大学大学院医学系研究科病態医科学講座免疫学分野・講師
2) OKADA Noriko　同分野・教授

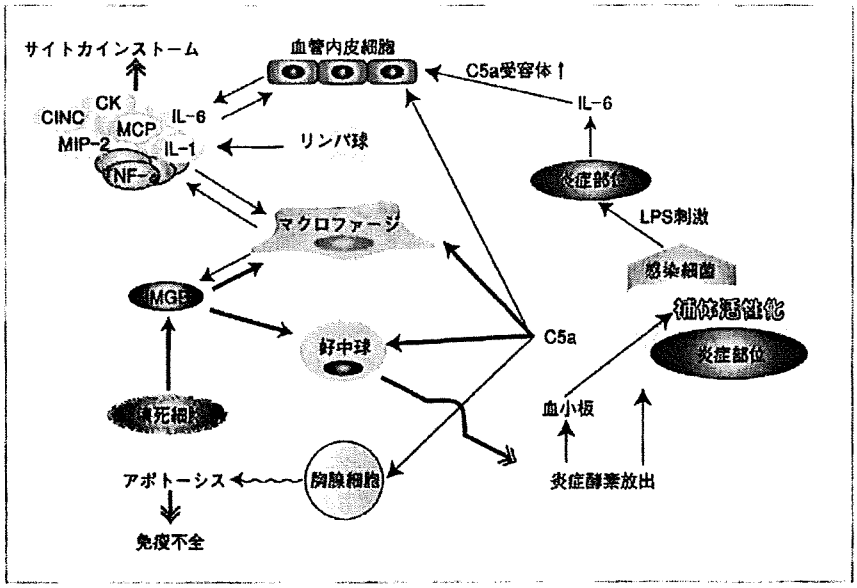

図2　C5a アナフィラトキシンの敗血症ショックにおける役割

スペプチド間でのハイドロパシーが逆相関値となることが知られている．AHB は対応するセンスペプチド間で相互作用することにより，高次構造の形成と維持に重要な働きをしているであろうことが推察された(図 1)．そこでわれわれは，AHB に対応する相補性ペプチドを設計，合成して作用させることにより，蛋白質の機能制御が可能となることを立証してきた．相補性ペプチドとは，標的ペプチドに対して，疎水性パターンが逆値になって相補性になっていること，対応する位置のアミノ酸側鎖の容積(bulkiness)が対応性でアミノ酸同士の α 炭素が 0.5 nm 以内に接近できること，ペプチド骨格のバックボーン並列性(backbone alignment)の一致性などを指標にして作成するペプチドであり，われわれは相補性ペプチドを自動設計するコンピュータプログラム MIMETIC を独自に開発することに成功した[2]．現在までに，MIMETIC で設計合成した相補性ペプチドの約 30% が標的蛋白質の機能を制御する活性をもち，相補性ペプチドの蛋白質機能制御の有効性が検証できており[3-5]，これらの中から最適な炎症過反応制御性ペプチドを選出して解析を進めている．

3. アナフィラトキシン C5a の機能

C5a(fifth component of complement)は補体活性化反応の中間産物であり，アナフィラトキシン(anaphylatoxin)と呼称されるごとく，血管透過性を高めてショック症状を引き起こす．また，極微量(pg オーダー)で単球やマクロファージを活性化して炎症局所に遊走集積させ，interleukin(IL)-1β，IL-6，tumor necrosis factor(TNF)-α などの炎症性サイトカインを分泌する．一方で，肥満細胞や好塩基球を活性化し，アレルギー性の炎症を引き起こすヒスタミンやセロトニンなど種々のメディエーターを放出させる．さらに，C5a は血管内皮細胞に直接作用し，P-セレクチンなどの接着分子を発現させる．C5a 刺激によりマクロファージから放出された IL-1β，TNF-α は血管内皮細胞表面に intercellular adhesion molecule(ICAM)-1 や E-セレクチンを，IL-6 は C5a レセプターの発現を増強させる．通常ではこのような免疫応答で炎症を引き起こされた後，炎症性サイトカインやそれらを放出するマクロファージ，好中球は時間の経過とともに沈静化されるが，過剰な炎症反応ではマクロファージや好中球，血管内皮細胞から大量の炎症性サイトカインが放出され，サイトカイン・ストームを誘発する(図 2)．敗血症などにおいては，細菌により宿主の正常な免疫応答力が阻害された免疫不全の状態にも陥り，DIC や MOF などの重篤な病態に進行

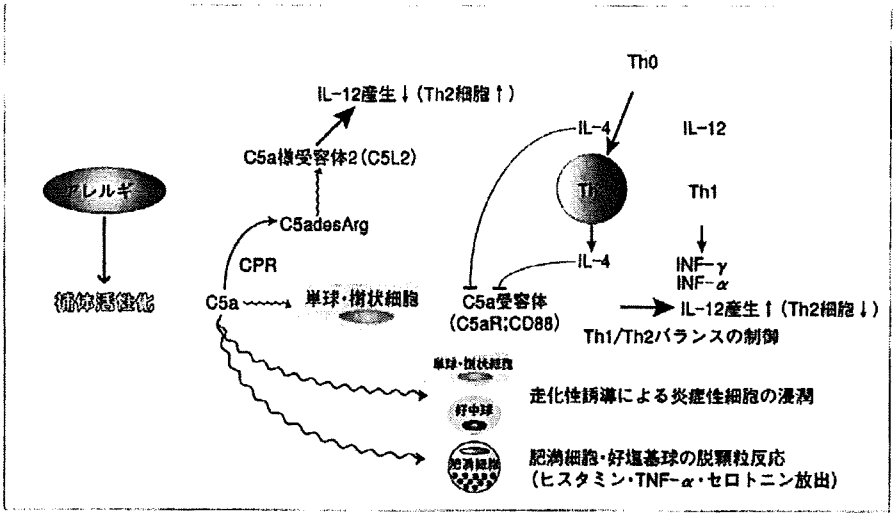

図3 アレルギー症状発症における C5a アナフィラトキシンの役割

すると考えられる[6].

4. C5a に対する相補性ペプチドのエンドトキシンショックに対する治療効果

Baranyi らは C5a と C5a 受容体に対する分子間 AHB を検索し，AHB ペプチドが C5a 刺激による細胞内へのカルシウムイオンの流入を抑制することを見いだし，C5a-C5a 受容体の相互作用に影響を及ぼすことを証明した[7]．その中で最も強い阻害活性を示した C5a の AHB ペプチドである PL37 に対する相補性ペプチドを MIMETIC で検索し，C5a に反応してその相互作用を阻害する相補性ペプチド PepA を創出した．LPS(lipopolysaccharide：リポ多糖)投与によるラットエンドトキシンショック実験モデルにおいて，コントロールでは生存率 0% であったのに対し，4 mg/kg の PepA を静脈注射すると全例を救命できた[4]．ペプチド剤は蛋白分解酵素の作用を受け，速やかに分解されるため半減期が短いという欠点がある．そこで，PepA の N 末端アミノ酸をアセチル化した AcPepA を作成して検討した結果，AcPepA はさらに強力な効果を発揮することが確かめられた[8]．さらに AcPepA は，致死量の LPS を投与したエンドトキシンショック病態のカニクイザルを救命できることも証明されており，臨床応用への道が開かれつつある．

5. C5a に対する相補性ペプチドの抗アレルギー効果

炎症性疾患の一つである喘息などのアレルギー病態にも，C5a アナフィラトキシンが深く関与している．Th2 細胞より放出されたサイトカインが B 細胞を刺激し，IgE 抗体を産生させる．IgE 抗体は好酸球や肥満細胞の受容体に結合し，そこに抗原が結合すると，ヒスタミンやセロトニンなどのメディエーターを放出させ炎症を引き起こす．アレルギー反応が補体系を活性化するメカニズムとして，アレルゲンが糖鎖構造をもっている場合は直接レクチン経路または第二経路で，アレルゲン—抗体複合体形成の場合は古典経路で活性化されることが知られている．補体の活性化により生じた C5a は好中球，単球，好酸球，肥満細胞，好塩基球や T 細胞などの炎症性の細胞に認識され，それらの細胞を炎症局所に集積させ，単球を樹状細胞へ分化誘導や，サイトカインおよびヒスタミンなどを放出させる．さらに，近年 C5a が抗原提示細胞を介して，T 細胞の Th1/Th2 反応を制御していることが明らかになってきた[9]．C5a は単球や樹状細胞上に発現している C5a 受容体に結合し，IL-12 を産生することにより Th1 反応を誘導するのだが，アレルギー症状のような Th2 優位の際は，Th2 細胞から産生される IL-4 により，単球や樹状細胞の C5a 受容体の発現を